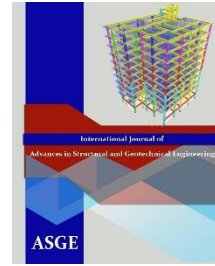




Egyptian Knowledge Bank



***International Journal of Advances in Structural
and Geotechnical Engineering***

<https://asge.journals.ekb.eg/>

Print ISSN 2785-9509

Online ISSN 2812-5142

Special Issue for ICASGE'19

***ENHANCEMENT OF TENSION LAP SPLICE IN
HPC USING DIFFERENT TECHNIQUES***

Tarek Fawzy, Abdel-Hakim Khalil, Ahmed Atta, Hamdy Afefy, and Mohamed Ellithy

ASGE Vol. 03 (02), pp. 77-92, 2019

ENHANCEMENT OF TENSION LAP SPLICE IN HPC USING DIFFERENT TECHNIQUES

Tarek Fawzy¹, Abdel-Hakim Khalil², Ahmed Atta³, Hamdy Afefy⁴,
Mohamed Ellithy⁵

¹Professor of concrete structures, Faculty of Engineering, Tanta University, Egypt.
E-mail: tarek.elshafi@f-eng.tanta.edu.eg

²Professor of concrete structures, Faculty of Engineering, Tanta University, Egypt.
E-mail: abdelhakeem.khalil@f-eng.tanta.edu.eg

³Professor of concrete structures, Faculty of Engineering, Tanta University, Egypt.
E-mail: AhmedAtta@f-eng.tanta.edu.eg

⁴Professor of concrete structures, Faculty of Engineering, Tanta University, Egypt.
E-mail: hamdy.afefy@f-eng.tanta.edu.eg

⁵Assistant lecturer, Structural Engineering Department, Faculty of Engineering, Tanta University, Egypt. E-mail: mohamed.ezat@f-eng.tanta.edu.eg

ABSTRACT

High Performance Concrete (HPC) with favorable material properties has been commonly used in different reinforced concrete projects such as bridges, tunnels, tall buildings and parking garages. Due to the limited lengths of manufactured reinforcement steel bars, splicing of these bars is urgently required for long span structures. Since lap splice is considered as the most economic and the easiest way for linking reinforcement steel bars, an experimental study on 21 lap splices embedded in HPC specimens was performed under direct tension test. Five different techniques were employed for straight and anchored bars with several splice lengths in order to obtain the minimum lap splice length for transferring the design force of the bars. For straight bars, spiral confinement with either inner or outer linking bars was used. On the other hand, for anchored bars, hooks, hooks with cross bars and end bearing plates were used. It was found that a splice length of $10 d_b$ was sufficient to achieve nominal yield stress of reinforcement in case of using spiral confinement with inner linking bars. On contrary, $5 d_b$ length of splice was found enough for all anchored bars to achieve their design force.

Keywords: Lap splice, High performance concrete, Direct tension, Anchored bars, Spiral confinement.

1. INTRODUCTION

The overall structural performance of reinforced concrete elements is mainly dependent on the bond characteristics between reinforcing steel bars and the surrounding concrete. Therefore, the adopted development lengths and lap splices of reinforcing steel bars have to be fully understood. Thus, this area of research has attracted the interest of many researchers worldwide. The governing parameters have been found to be the concrete type/strength, reinforcing bar diameter, concrete cover, method of splicing of bars, confinement of bars, coating of bars and loading type.

Since the type of concrete is an effective parameter, using Ultra-High-Performance Fiber Reinforced Concrete (UHPFRC) showed a considerable improvement on bond performance and splitting crack control. For UHPFRC mix having fiber volumetric ratio of 4%, a splice length of $12 d_b$ was found to be sufficient for achieving yield for 400 MPa reinforcement [1]. Also, Strain-Hardening Cementitious Composite (SHCC) mixtures was found to be effective in reducing the development length of rebar up to 60 percent of the splice length required by the ACI 318 equation according to splitting failure controlled by multiple cracking behavior of SHCC mixtures [2]. Fiber Reinforced Cement Composites (FRCC) showed that the fibers induced bridging effect after cracking can effectively support post-cracking tensile capacity to the concrete matrix and limit crack width, thereby leading to enhanced bond resistance [2,3,4,5]. The effectiveness of UHPFRC for strengthening deficient lap splices was tested in 18 full-scale beam specimens. Splitting failure in the lap splice region was completely eliminated due to the high tensile strength and energy absorption capabilities of the used UHPFRC [6]. Furthermore, splice length of deformed bars embedded into high-strength self-compacted concrete beams were examined [7]. A splice length of 40 times bar diameter was found the minimum splice length to be taken as a sufficient splice length since beams started cracking and failed at a load equal or higher than those without splice [7]. Researches have also proved that the bond behaviour and failure modes were noticed to be similar in the natural and the recycled aggregate concrete [8].

Regardless of concrete type, the failure of specimens with lap splices without transverse reinforcement was violent and occurred along the entire length of the splice. Adding proper confinement along the splice zone improved the behavior as the proper confinement eliminated the formation of splitting cracks at tension splice zone [9,10,11]. Several techniques were used in order to strengthen the ordinary lap splice such as welding, headed bars and hooks. The main idea of hooks and headed bars is to use anchors at the end of steel bars which provides higher resistance for reinforcing bars against slippage. Although welded splicing reduces rebar congestion and improves concrete consolidation, it requires special labor and equipment which entails additional cost [12]. Headed bars can transfer the bar full strength to concrete with only $4d_b$ splice length [13]. Therefore, headed bar could be considered as an effective way to minimize the lap splice length but it still not practical method in narrow elements with adjacent lapped bars. Equations were

ICASGE'19

25-28 March 2019, Hurghada, Egypt

developed to estimate the anchorage strength of hooked bars with and without confining reinforcement. The equations are based on test results of 245 simulated beam-column joint specimens [14].

Lap splice is considered the most economic and the easiest way for splicing the reinforcing steel bars. Accordingly, the current research is devoted to develop and study the behavior of different lap splicing techniques aiming to increase their capacity as well as minimizing the lap splice length.

2. EXPERIMENTAL INVESTIGATION

2.1 Test specimens and studied parameters

In the current study, the specimens are two pairs of lap spliced 12 mm diameter bars in HPC prism with/without transverse reinforcement and were axially loaded by tension force. The tested specimens were categorized into two different groups according to the configuration of the steel bars. Group 1 consisted of three different subgroups of straight bars with/without transverse steel as depicted in Fig. 1 to Fig. 3, while Group 2 presented three varied subgroups of anchored bars without confining reinforcement as shown in Fig. 4 to Fig.6. The steel bars of Group 2 were anchored by miscellaneous configurations, steel plate and 180° ACI 318 standard hook [15] were used as anchors as shown in Fig. 7 and Fig. 8. Table 1 summarizes the concrete prism dimensions and lap lengths for each subgroup.

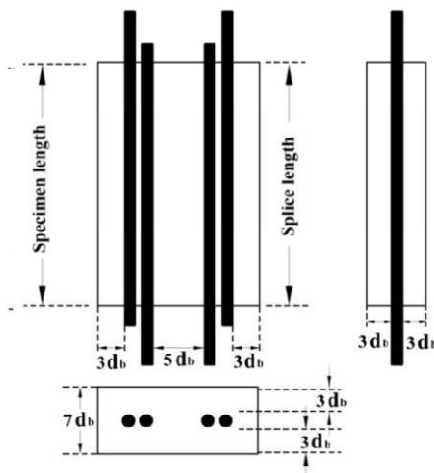


Fig. 1 Configuration of Group (1-O), ordinary lap splice.

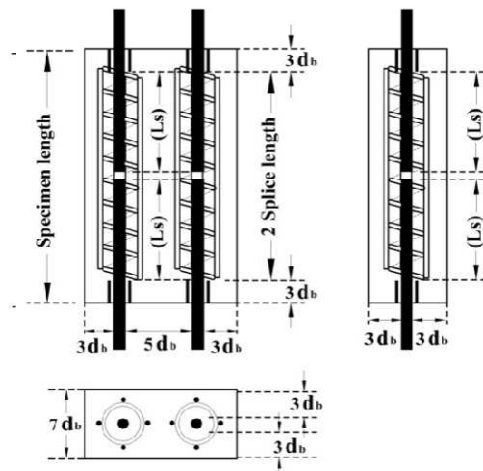


Fig. 2 Configuration of Group (1-SO), spiral confinement with outer linking bars.

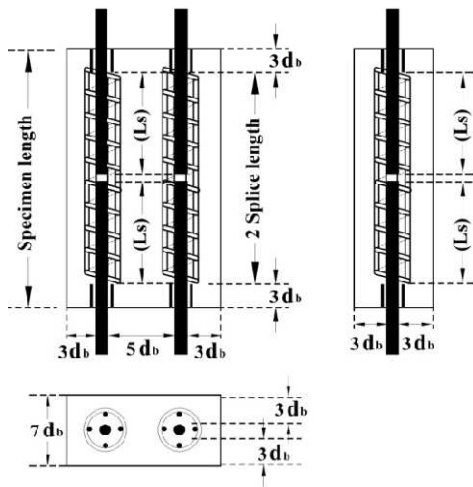


Fig. 3 Configuration of Group (1-SI), spiral confinement with inner linking bars.

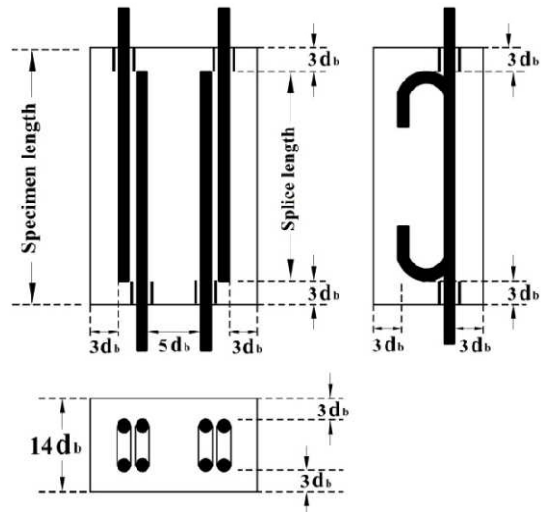


Fig. 4 Configuration of Group (2-H), standard 180° ACI-318 hook.

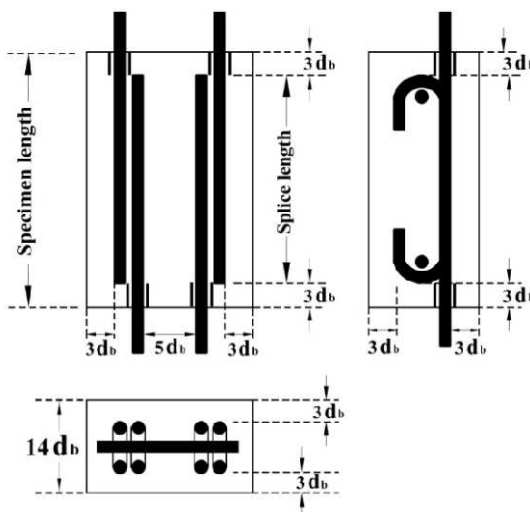


Fig. 5 Configuration of Group (2-HC), standard 180° ACI-318 hook with cross-bar.

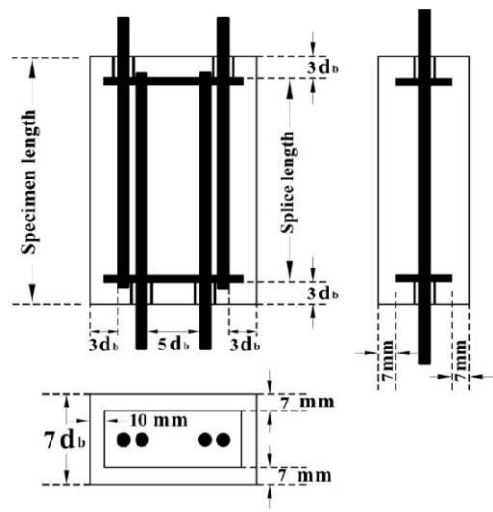


Fig. 6 Configuration of Group (2-P), end bearing plate.

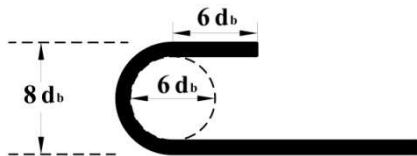


Fig. 7 ACI-318 standard hook of 180°.

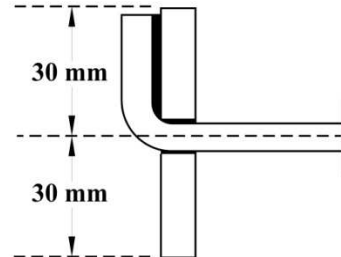


Fig. 8 Steel plate in which the bar is welded to the rear face .

Table 1 Specimens notations and dimension

Group	Sub-group	Splice length	Specimen notation	Prism dimensions (mm)		
				Length	Width	Depth
G1	O	10 d_b	G1-O-10d	120	180	84
		20 d_b	G1-O-20d	240	180	84
		30 d_b	G1-O-30d	360	180	84
	SO	10 d_b	G1-SO-10d	310	156	84
		20 d_b	G1-SO-20d	550	156	84
		30 d_b	G1-SO-30d	790	156	84
SI	10 d_b	G1-SI-10d	310	156	84	
	20 d_b	G1-SI-20d	550	156	84	
	30 d_b	G1-SI-30d	790	156	84	
G2	H	05 d_b	G2-H-05d	130	180	170
		10 d_b	G2-H-10d	190	180	170
		20 d_b	G2-H-20d	310	180	170
		30 d_b	G2-H-30d	430	180	170
	HC	05 d_b	G2-HC-05d	130	180	170
		10 d_b	G2-HC-10d	190	180	170
		20 d_b	G2-HC-20d	310	180	170
		30 d_b	G2-HC-30d	430	180	170
	P	05 d_b	G2-P-05d	130	180	84
		10 d_b	G2-P-10d	190	180	84
		20 d_b	G2-P-20d	310	180	84
		30 d_b	G2-P-30d	430	180	84

The adopted notation system of specimens shows the various testing parameters; where for specimen Gx-y-zd, "x" indicates the group, "y" refers to the subgroup and "z" is the splice length in term of bar diameter. Spiral stirrup of 6 mm bar diameter and inner spiral diameter of 40 mm with uniform pitch of 30 mm was used as transverse reinforcement for subgroups SO and SI. Four linking bars of 8 mm diameter were used for each specimen of SO and SI to ensure transformation of the maximum potential force among the tested specimens. The back of the

anchors was covered by concrete with length of $3d_b$, in this zone the bars were isolated to maintain the splice length between anchors. The configuration of specimens in the current study was adopted in several previous researches, which allows testing of full length lap splice without execution of full-scale beam splice specimen. The bond strength obtained by this configuration lays between 90% and 100% of what obtained by beam splice specimens with same conditions [1,16,17]. In this research the minimum concrete cover was deliberately selected $3d_b$ for all test specimens. The chosen concrete cover is common in practice in RC beams in the Middle East.

2.2 Steel bars properties

The nominal yield strength of reinforcing bars was 400 MPa for deformed bars and 280 MPa for smooth bars as typically used in the Middle East. For each bar diameter, four samples were collected from 12 mm and 8 mm diameter bars and were tested in accordance with ASTM A370 [18]. The average mechanical properties and geometries of the tested samples are listed in Table 2.

Table 2 Steel bars geometries and mechanical properties

Property	Splice bar	Linking bar
Nominal diameter, d_b (mm)	12	8
Core diameter, D (mm)	12	8
Average rib depth, h_r (mm)	0.9	-
Rib spacing, s_r (mm)	8.5	-
Rib face angle, θ ($^\circ$)	37	-
Relative rib area, R_r	0.1125	-
A_b (mm ²)	114.7	50.26
Young modulus, E_s (GPa)	207	203
Yield strength, f_y (MPa)	463	291
Ultimate strength, f_u (MPa)	631	453

2.3 HPC material properties

The HPC mix was the same for all tested specimens, the mix shows a self-consolidating behaviour allowing an excellent workability with light vibration. The concrete mix performed in the current research was the same mix used in a previous research [19]. The concrete mix is summarized in Table 3 where the water-to-cement ratio was 0.3. Precautions were taken to ensure bars alignment among the wood forms during casting. The current HPC mix showed well consolidation and was poured with light vibration. After casting, specimens were

covered by wet textile then curing process began and continued for six days. Material tests of HPC were performed at the same day of the lap splice test.

Table 3 Concrete mix design of HPC (kg/m³)

Cement	Water	Sand	Dolomite	Silica fume	Super plasticizer	Polypropylene fibers
450	135	535	1279	45	4.5	1.8

Compressive strength f_c' was determined from 150 x 300 mm standard cylinders according to ASTM C39 [20]. Brazilian test was performed to obtain the tensile strength f_t of HPC. Two cylindrical samples for each subgroup were tested to determine the compressive and tensile strengths at the day of testing the splice specimens of the same subgroup. To ensure early gained strength, one cylinder sample was tested, the 7 days age compressive strength was 40.1 MPa. Table 4 reports HPC main characteristics regarding to each lap splice specimen.

Table 4 HPC material properties

Subgroup	Age (days)	f_c' (MPa)	f_t (MPa)
G1-O	28	54	4.7
G1-SO	32	55	4.7
G1-SI	36	55	5.1
G2-H	40	54	4.9
G2-HC	43	56	4.9
G2-P	54	58	5.1

2.4 Instrumentation

One strain gauge outside the specimen for each lap splice bar was mounted to determine the strain in each bar during the test. A total of 4 LVDT (Linear Variable Differential Transformer) with a 50 mm gauge length were installed on the concrete surface at $4d_b$ from each end on the specimen front faces, perpendicularly to the axis of the splice joint as depicted in Fig. 9. The faces were sprayed with white colour to have a clearer view of the cracks took place on the surface of the specimens. MTS actuator was used to apply tension force and its outputs (load-displacement) were recorded. The failure of specimens is sudden and violent, thus, tests were recorded by slow-motion HD video camera with 120 fps.

ICASGE'19

25-28 March 2019, Hurghada, Egypt

2.5 Test setup

Splice bars were fixed to a rigid steel cap system via steel grips and wedges to ensure that both lapped bars were subjected to the same displacement. The rigid capping system was tested against bare bars, the cap deformation was inferior to 0.3 mm. To assure the best fitting of the bars with grips, the specimens were preloaded to 5 kN then released before testing. The rigid cap was attached to the thick platen of MTS actuator. Loading was applied by force control of the two top bars with a constant load rate 5 kN/min until failure. During the test, actuator output data was exported to a data-logger with sampling frequency 2 Hz. Fig. 9 presents the specimen, the instrumentation and the experimental set-up.



Fig.9 Test setup and instrumentation.

3. RESULTS AND DISCUSSION

3.1 Overall behaviour

Test results at maximum load for all tested lap splice specimens are summarized in Table 5. The maximum steel stress at failure f_s represents the average stress developed at the reinforcing bars. Bars stress is the output of dividing the maximum force by the average cross section of steel bars. Weight and length measurements were used to calculate the average cross section A_b of steel bars as shown in Table 2. To allow all subgroups to be compared with the reference subgroup G1-O, the ratio between $\sqrt{f_c}'$ of each subgroup and $\sqrt{f_c}'$ of G1-O was used to normalize the obtained steel stress f_{sn} . The maximum normalized steel stress was compared to the actual yield strength of steel in term of f_{sn} / f_y to calculate the efficiency of splice E_f .

Table 5 Test results of lap splice specimens

Group	Sub-group	Specimen notation	Max. Load (kN)	f_s (MPa)	f_{sn} (MPa)	E_f (f_{sn} / f_y)	Mode of failure
G1	O	G1-O-10d	60.9	265	265	0.58	P
		G1-O-20d	118.7	517	517	1.12	YP
		G1-O-30d	132.1	576	576	1.25	YP
	SO	G1-SO-10d	88.4	385	381	0.83	P
		G1-SO-20d	129.5	565	560	1.22	YP
		G1-SO-30d	140.3	612	606	1.32	YP
	SI	G1-SI-10d	97.2	424	420	0.91	P
		G1-SI-20d	149.7	653	647	1.41	R
		G1-SI-30d	145.3	633	627	1.36	R
G2	H	G2-H-05d	99.5	434	434	0.94	SH
		G2-H-10d	118.7	517	517	1.12	SH
		G2-H-20d	132	575	575	1.25	YPC
		G2-H-30d	133.2	581	581	1.26	YPC
	HC	G2-HC-05d	109.8	479	470	1.02	YPC
		G2-HC-10d	143.3	625	614	1.33	YPC
		G2-HC-20d	136.1	593	582	1.27	R
		G2-HC-30d	139	606	595	1.29	R
	P	G2-P-05d	145.5	634	612	1.33	R
		G2-P-10d	145.2	633	611	1.33	R
		G2-P-20d	138.6	604	583	1.27	R
		G2-P-30d	142.4	621	599	1.3	R

P : Pullout/slippage of reinforcing bars.

YP : Yielding of steel followed by pullout/slippage of bars.

YPC : Yielding of steel followed by pullout/ slippage of bars then concrete crushing.

R : Rapture of reinforcing bars.

SH : Direct shear on the plane of intersection of hooked lapped bars.

For G1 specimens, the specimens of G1-O exhibited the lowest efficiency than those of other subgroups with the same lap lengths due to absence of confinement. Although G1-SO is easier in implementation than G1-SI, the later showed higher loads because its linking bars had inferior concrete cover and were located out of the confined zone. The minimum lap length can transfer the nominal yield strength of G1 specimens was recorded by G1-SI-10d, however, the other specimens of G1 needed $20d_b$ at least to reach yielding strength of reinforcing bars. Due to anchoring techniques in specimens of G2, their capacities enhanced than those of the same lap lengths of G1. Using cross-bar with hooked reinforcement had an obvious effect not only on the efficiency but also on the mode of failure. All specimens of G2-P achieved the maximum strength of steel and recorded rupture of reinforcing bars. It only requires just $5d_b$ for specimens of G2 to attain the nominal design force of reinforcing bars.

3.2 Mode of failure

Shear crack and/or local concrete crushing due to bar pullout was noted for all specimens of G1-O as shown in Fig. 10. The failure of G1-O-10d was prior to yielding of steel bars and the other specimens of G1-O failed after yielding. Splitting cracks were not obvious during testing and appeared only at the time of failure.

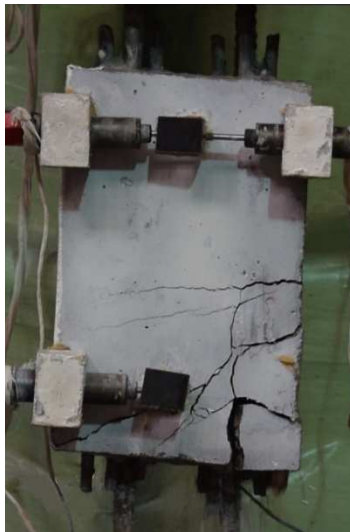


Fig. 10 Bars pullout of G1-O-20d.

ICASGE'19

25-28 March 2019, Hurgada, Egypt

Owing to the inferior concrete cover, all specimens of G1-SO failed due to slippage of the outer linking bars which located out of the confined zone. Relocation of linking bars inside the spiral stirrup of G1-SI changed not only splice efficiency but also mode of failure. G1-SI-10d presented pullout of main bars of 12 mm diameter, the linking bars did not slip due to the effect of confinement and the superior concrete cover. Other specimens of G1-SI showed the maximum capacity and reached rupture of steel bars. Mode of failure of specimens from G1-SO and G1-SI is shown in Fig. 11.



(a) pullout of 12 mm diameter bars of G1-SI-10d.



(b) slippage of outer linking bars of G1-SO-10d.

Fig. 11 Mode of failure of specimens (a) G1-SI-10d and (b) G1-SO-10d.

Using anchoring techniques for G2 changed the manner of specimens and consequently the mode of failure. For 5 and 10 d_b lap splice of G2-H, a unique failure mode was noted, direct shear failure on the plane of intersection of hooked lapped bars. For 20 and 30 d_b of G2-H the area of shear plane was much bigger, thus a different mode of failure was recorded, pullout of bars followed by crushing of concrete. Using cross bars in G2-HC perpendicular to the intersecting hooked lapped bars prevented creation of direct shear plane and enhanced load capacity of specimens than that of G2-H. Fig. 12 shows the front face of G2-H-10d and the direct shear plane from the side view. For specimen G2-HC-10d, Fig. 13 presents the concrete block created after failure due to the cross bar effect, preventing the direct shear failure.



(a) side view of G2-H-10d showing direct shear plane of failure



(b) Front face of G2-H-10d showing direct shear plane of failure

Fig. 12 Direct shear plane of failure of G2-H-10d.



Fig. 13 concrete block formed after failure of G2-HC-10d.

Developing an innovative technique of end bearing plate for G2-P led to the same mode of failure for all subgroup specimens. The specimens of G2-P showed rupture of reinforcing bars with maximum potential strength of steel. During testing of G2-P specimens, the movable plates converted the tension force of bars into compression force acting on concrete in front of the plate. This action played a role of reducing the direct tension cracks of concrete during testing especially in short lap splice specimens G2-P-5d and G2-P-10d which remained without cracking until failure. Fig. 14 shows the compression force created on the face of bearing plates.

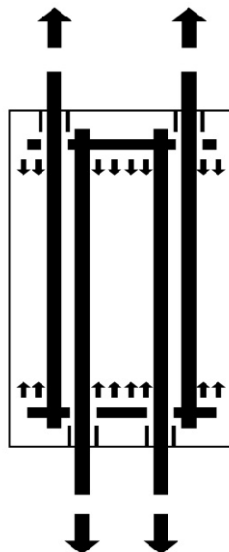


Fig. 14 Compression force acting on concrete at the face of bearing plates.

4. Conclusions

The main objective of this paper was to experimentally investigate different techniques to enhance the lap splice in HPC prism under direct tension. The test specimens consisted of two pairs of spliced bars in a HPC prism with/without confining reinforcement. Five different techniques and four different splice lengths were performed to develop practical methods to minimize the ordinary lap splice. Based on the experimental outputs of the current study, the following notes can be concluded.

- Generally, the specimens of G1-O showed the lowest load capacities than those of other subgroups of G1 owing to absence of confinement. All specimens of G1-O failed due to slippage of steel bars followed by concrete crushing.

- The configuration of G1-SO is easier and more practical than G1-SI but the later showed higher splice efficiency. G1-SI-10d showed 10% higher load than G1-SO-10d and both of them failed prior to reaching the yield strength. The other specimens of G1-SI failed by rupture of 12 mm diameter bars, while the same specimens of G1-SO failed due to slippage of linking bars of 8 mm diameter.
- During testing, the linking bars of G1-SI sustained without slippage because it were inside the confined zone with larger concrete cover than that of G1-SO.
- For specimens of G1-SI, only $10 d_b$ was sufficient to achieve the nominal yield stress (400 MPa), while the longer splice lengths achieved the ultimate steel capacity.
- Using cross bars with G2-HC of 5 and $10 d_b$ splice lengths raised the capacity by 10% and 20% respectively than those of G2-H and changed their mode of failure. The cross bars were perpendicular to the spliced hooked bars and intersecting with the direct shear plane which prevent it from creation.
- Rupture of reinforcing bars was attained by all specimens of G2-P with innovative technique of end bearing plates. Specimens G2-P-5d and G2-P-10d remained without cracking during testing owing to the action of plates which converted the tension force of bars into compression force acting on concrete in front of the plates.

ACKNOWLEDGEMENT

The experimental work was performed in the Reinforced Concrete and Heavy Structures Laboratory of Faculty of Engineering, Tanta University, Tanta, Egypt.

REFERENCES

- [1] Lagier, F., Massicotte, B. and Charron, J., (2015), "Bond strength of tension lap splice specimens in UHPFRC", *Construction and Building Materials* Vol. 93, pp. 84–94.
- [2] Choi, W., Jang, S. and Yun, H., (2016), " Bond and cracking behavior of lap-spliced reinforcing bars embedded in hybrid fiber reinforced strain-hardening cementitious composite (SHCC)", *Composites Part B*.
- [3] Dagenais, M. and Massicotte, B., (2017), " Cyclic Behavior of Lap Splices Strengthened with Ultrahigh Performance Fiber-Reinforced Concrete", *Structural Engineering*, Vol. 143 (2).
- [4] Marchand, P., Baby, F., Khadour, A., Battesti, T., Rivillon, P., Quiertant, M., Nguyen, H., Gre'gory Ge'ne'reux, Deveaud, J., Simon, A., and

ICASGE'19

25-28 March 2019, Hurghada, Egypt

- Toutlemonde, F., (2016), "Bond behaviour of reinforcing bars in UHPFRC", *Materials and Structures*, Vol. 49, pp. 1979–1995.
- [5] Metelli, G., Marchina, E., Plizzari, G.A., (2017), "Experimental Study on Staggered Lapped Bars in Fiber Reinforced Concrete Beams", *Composite Structures*.
- [6] Dagenais, M. and Massicotte, B., (2015), "Tension Lap Splices Strengthened with Ultrahigh-Performance Fiber-Reinforced Concrete", *Materials in Civil Engineering*, Vol. 27 (7).
- [7] El-Azab, M., Mohamed, H. and Farahat, A., (2014), "Effect of tension lap splice on the behavior of high strength self-compacted concrete beams", *Alexandria Engineering Journal*.
- [8] Prince, M., Gaurav, G. and Singh, B., (2018), "Splice strength of deformed steel bars embedded in recycled aggregate concrete", *Construction and Building Materials*, Vol. 160, pp. 156–168.
- [9] Garcia, R., Helal, Y., Pilakoutas, K. and Guadagnini, M., (2014), "Bond behaviour of substandard splices in RC beams externally confined with CFRP", *Construction and Building Materials*, Vol. 50, pp. 340–351.
- [10] Hamad, B., Ali, A. and Harajli, M., (2005), "Effect of Fiber-Reinforced Polymer Confinement on Bond Strength of Reinforcement in Beam Anchorage Specimens", *JOURNAL OF COMPOSITES FOR CONSTRUCTION*, Vol. 9(1), pp. 44-51.
- [11] Mabrouk, R. and Mounir, A., (2017), " Behavior of RC beams with tension lap splices confined with transverse reinforcement using different types of concrete under pure bending", *Alexandria Engineering Journal*.
- [12] Issa, C.A. and Nasr, A., (2006), "An experimental study of welded splices of reinforcing bars", *Building and Environment*, Vol. 41, pp. 1394–1405.
- [13] Vella, J. P., Vollum, R. L., and Jackson, A., (2017), " Investigation of headed bar joints between precast concrete panels", *Engineering Structures*, Vol. 138, pp. 351–366.
- [14] Sperry, J., Darwin, D., O'Reilly, M., Lequesne, R. D., Yasso, S. Matamoros, A., Feldman, L. R. and Lepage, A., (2017), "Conventional and High-Strength Hooked Bars— Part 2: Data Analysis", *ACI Structural Journal* Vol.114, No.1, pp.267-276.
- [15] ACI 318-14, (2014), "Building Code Requirements for Structural Concrete", ACI committee 318, American Concrete Institute.
- [16] Burkhardt, C., (2000), "Behavior of lap splices in high strength concrete", [Ph.D thesis], Aachen, Germany: RWTH Aachen University; p. 190 [in German].
- [17] Richter, B., (2012), "A new perspective on the tensile strength of lap splices in reinforced concrete members", [M.Sc thesis], West Lafayette, USA Purdue University, p. 165.
- [18] ASTM, 2010, Standard test methods and definitions for mechanical testing of steel products – Annex A9 methods for testing steel reinforcing bars. A370. ASTM West Conshohocken, PA, USA.



- [19] Horszczaruk, E.K., (2009), "Hydro-abrasive erosion of high performance fiber-reinforced concrete", *Wear* Vol.267, pp.110-115.
- [20] ASTM, 2010, Standard test method: compressive strength of Cylindrical Concrete Specimens, C39/C39M. ASTM West Conshohocken, PA, USA.